

Evaluating Tree-Ring Proxies For Ecosystem Productivity In India Through Observations And Model Products

A Master's Thesis

submitted to

Indian Institute of Science Education and Research, Pune

in partial fulfilment of the requirements for the

BS-MS Dual Degree Program

By

Aharna Sarkar

Roll no. 20181121



Indian Institute of Science Education and Research, Pune

Dr. Homi Bhabha Road,

Pashan, Pune 411008, INDIA

10th April, 2023

Supervisor: Dr. Supriyo Chakroborty

Indian Institute of Tropical Meteorology, Pune

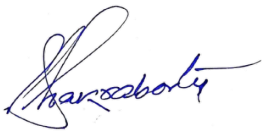
Co-Supervisor: Dr. Prमित Kumar Deb Burman

Centre for Climate Change Research

Indian Institute of Tropical Meteorology, Pune

CERTIFICATE

This is to certify that the dissertation entitled “***Evaluating Tree-Ring Proxies For Ecosystem Productivity In India Through Observations And Model Products***” towards the partial fulfilment of the BS-MS dual degree program offered at Indian Institute of Science Education and Research, Pune, represents work carried out by Aharna Sarkar at Indian Institute of Science Education and Research, Pune, under the supervision of Dr. Supriyo Chakroborty, Retired Scientist, Indian Institute of Tropical Meteorology, Ministry of Earth Sciences and Dr. Prमित Kumar Deb Burman, Scientist D, Centre for Climate Change Research, Indian Institute of Tropical Meteorology, Ministry of Earth Sciences, during the academic year 2022-2023.



Dr. Supriyo Chakroborty
Scientist-F (Retired)
Indian Institute of Tropical Meteorology, Pune



Dr. Prमित Kumar Deb Burman
Scientist-D
Centre for Climate Change Research
Indian Institute of Tropical Meteorology, Pune

DECLARATION

I hereby declare that the research work presented in the report entitled “***Evaluating Tree-Ring Proxies For Ecosystem Productivity In India Through Observations And Model Products***” has been carried out by me at the Department of Earth and Climate Sciences, Indian Institute of Science Education and Research, Pune, under the supervision of Dr. Supriyo Chakraborty and Dr. Prमित Kumar Deb Burman and the same has not been submitted by me elsewhere for any other degree.



Aharna Sarkar

20181121

BS-MS

IISER Pune

ACKNOWLEDGEMENT

Foremost, I would like to extend my sincere gratitude to my supervisors, Supriyo sir and Pramit sir, for their patience, guidance, and for pushing me to think outside the box in tackling the scientific problem at hand. Even when my results seemed nonsensical, they remained supportive and committed to helping me progress. I would also like to express my appreciation to Dr. Hemant P. Borgaonkar, whose keen interest in my project and invaluable expertise in the field led us towards the right direction. Additionally, I thank Dr. Deepak Barua for his guidance throughout the thesis evaluation process and his valuable inputs on my work. I am grateful to IISER Pune for providing me with the opportunity to undertake a year-long independent project, which has been a transformative experience that has positively impacted my research career.

The past year has been a rewarding journey, filled with both academic and personal challenges, and I would like to express my gratitude to the organisations and individuals who have positively impacted my experience. Firstly, I would like to thank Science Gallery Bangalore for providing me with the opportunity to participate in a month-long summer camp on Carbon and Climate Change. The camp enriched my research work, provided me with valuable insights, and equipped me with the necessary resources to tackle the problem at hand. I am also grateful to the administration of the Indian Institute of Tropical Meteorology (IITM) for hosting me as a project student. Special thanks to Dr. Naveen Gandhi and the Development of Skilled Manpower (DESK) at IITM for allowing me to attend the National Training Workshop on Paleoclimate - Archives, Proxies, and Analysis/Measurement Techniques. This workshop was particularly timely, as I had hit a plateau in my thesis work. During the six-day workshop, I had the opportunity to interact with multiple experts and peers working on a wide range of paleoclimate problems. I learned about the best practices in the field and gained the motivation necessary to push forward with my research work.

I would like to express my heartfelt gratitude to Dr. Saikrishnan Kairat, the Dean of Student and Campus Activities, for believing in me and allowing us to organise the

Inter-IISER Cultural Meet (IICM) in December 2022. This was by far the most challenging extracurricular task I had undertaken in my five years at IISER. The experience taught me invaluable people and time management skills, especially as I juggled the event alongside my research work. I am also deeply grateful to my unwavering pillars of support - *Maa, Baba and Dada* - who have encouraged me in all my endeavours since birth. Their faith in me, even during moments of self-doubt, has helped me push forward. I would also like to thank my dear friends Ningnung, Srijay, Srishti, and Sultan for making my time at IISER memorable and participating in IISER activities, even when they did not necessarily want to, just to support me. My dearest Rakshit deserves a special mention for his love and care throughout my final year at IISER. He has been a sounding board for many of my project ideas, and his unwavering support was critical during the last few months of my thesis work when I faced serious health issues. Lastly, but not in the least, I am grateful to the Department of Science and Technology for electing me as a beneficiary of the Inspire-SHE fellowship.

CONTENTS

1. List of Figures	7
2. List of Tables	8
3. List of Acronyms	8
4. Abstract	9
5. Introduction	10 - 13
6. Data and Methods	14 - 22
7. Results and Discussion	23
7.1. CMIP6 model validation	23 - 27
7.2. Tree ring analysis	27 - 38
8. Conclusion and Future scope	39 - 40
9. References	41 - 47

LIST OF FIGURES

1. Map of India showing the tree ring sites used in the study.....	18
2. Taylor diagram comparing the performance of test datasets of gross primary productivity output from ACCESS-ESM1.5 and NorESM2-LM with MODIS GPP product as reference dataset.....	23
3. Multi-year monthly mean from January 2000 to December 2014 for the NWH region of ecosystem carbon flux variables for the CMIP6 models and MODIS GPP.....	24
4. Multi-year monthly means of daily GPP of a forest site in Betul, Madhya Pradesh.....	25
5. A scatter plot of GPP-RA vs NPP for the model outputs from January 2000 to December 2014 is shown.....	26
6. Basal area increment and ring width index plotted for Ghansali.....	30
7. Chronologies of BAI and BAI Ar 1 plotted with annual ACCESS GPP to check overall correlation between the series.....	31
8. Two sample tree ring cores from Ghansali showing the increased peak at the end and the standardised values.....	31
9. Multi-year monthly mean of NPP, GPP and RA values from ACCESS-ESM1.5 for Ghansali for the period 2000-2014.....	32
10. Growing season of <i>Pinus roxburghii</i> is indicated by the high positive correlation of the month's GPP with the annual tree ring index (BAI or RWI).....	33
11. Relative importance of variables in explaining the variance in BAI for Ghansali.....	34
12. Pearson correlation of monthly NPP and GPP with annual BAI.....	36
13. Relative importance of variables in explaining the variance in BAI and RWI for the NWH region.....	38

LIST OF TABLES

1. Comparison of model descriptions of CSIRO's ACCESS-ESM1.5 and NCAR's NorESM2-LM.....	15
2. Information on the tree ring sites used in the study.....	18
3. Performance of various detrended series as a proxy for tree growth tested against annual sums of NPP and GPP from ACCESS-ESM-1.5	27
4. BAI statistics from the study sites. Mean, standard deviation (SD), standard error (SE) and average year to year change in BAI.....	29
5. Granger causality test results for the Ghansali site.....	33
6. Incremental pseudo R2 (% variance explained) values of each variable when added to regression models. BAI was the target variable.....	34
7. Inter-site Pearson correlations of the Cedrus deodara trees.....	35
8. Pearson correlation coefficients of the individual sites with their annual NPP and GPP and of the NWH region with the regional average of the annual NPP and GPP series.....	36
9. Incremental pseudo R2 (% variance explained) values of each variable when added to regression models for the NWH region with BAI as the target variable.....	38
10. Incremental pseudo R2 (% variance explained) values of each variable when added to regression models for the NWH region with RWI as the target variable.....	38

LIST OF ACRONYMS

AC - Autocorrelation
AWB - Above-ground woody biomass
BAI - Basal area increment
EC - Eddy covariance
GPP - Gross primary productivity
NEE - Net ecosystem exchange
NEP - Net ecosystem productivity
NPP - Net primary productivity
RA - Autotrophic respiration
RWI - Ring width index

ABSTRACT

Terrestrial ecosystems are one of the major sinks of atmospheric CO₂ and play a key role in climate change mitigation. They also modulate the local climate by exchanging scalar, energy, and momentum with the atmosphere. On the other hand, the ecosystem-atmosphere interactions are also modulated by climate variability. For example, depending on the environmental parameters, plant carbon synthesis and the allocation of assimilated carbon into its different biomass pools, such as roots, trunks, leaves, etc. Several studies have focused on understanding the carbon sequestration processes in terrestrial ecosystems and their response to climate change. Most of these studies have used the Eddy Covariance (EC) technique to measure the ecosystem-atmosphere carbon, water and energy fluxes. However, very few of them address the linkage of tree-ring growth with the ecosystem-atmosphere carbon exchange. EC has been a fairly advanced technique, and these studies span the last few decades at the most. Particularly for India, the EC flux records do not extend beyond the last decade. However, the tree-ring records typically extend up to a few centuries and may capture long-term climate variability's effects on carbon sequestration in forest ecosystems. We study the Coupled Climate Carbon Cycle Model Intercomparison Project (C4MIP) model outputs (a project under CMIP6) for its 165-year-long simulated records of mainly mean monthly gross primary productivity (GPP) and net primary productivity (NPP) and compare them with the tree-ring growth indices over the northwestern Himalayan region. Through their correlations with other climate variables, and their statistical correlation measures, we establish confidence in tree-ring growth indices as proxies for reconstructing aboveground woody biomass and estimating ecosystem productivity.

INTRODUCTION

The prevailing scientific view is that the rise in concentrations of greenhouse gases (GHGs) and accompanying feedback processes leading to radiative processes are the main causes of global warming and climate change (IPCC 2013). Of all the anthropogenic greenhouse gases, the heightened levels of atmospheric carbon are particularly worrisome as CO₂ remains in the atmosphere for an extended period, up to 100 years (IPCC 2013). The sixth assessment report of IPCC (2021), with high confidence, has stated that Carbon Dioxide Removal (CDR) plays a crucial role in the scenarios aimed at restricting global warming to 2°C (>67%) or 1.5°C (>50%) by the year 2100. The report also mentions afforestation as one of the cheapest, readily available and most efficient CDR methods.

Forest ecosystems function as a carbon (C) sink that offsets ~ 25% of the annual anthropogenic C emissions, thereby playing an active role in mitigating climate change. The total C stock in any forest ecosystem is derived from aboveground biomass (AGB) or leaves, trunk, branches, belowground biomass (BGB) or roots, forest floor litter biomass (LB) or detritus pool, wood debris, and soil organic matter (SOM) as per IPCC guidelines. C allocation to these pools is controlled by various factors like climate, forest management practices, tree age, tree physiology, land use change, forest disturbances, nutrient and light competitions and intensive seed production (Babst et al., 2013). The allocation of C to the aboveground wood biomass (AWB) or tree trunks and branches is the most significant contributor to the storage of C in vegetation over time frames relevant to the climate (Capon et al., 2022). Thus, assessing the amount of carbon stored in various pools, especially in AWB is essential for devising new conservation policies aimed at carbon sequestration and mitigating the effects of climate change (Pant and Tiwari, 2014 and Meena et al., 2019).

The C uptake by a forest ecosystem or its carbon sequestration potential can also be measured in terms of carbon fluxes at the canopy height of the ecosystem (Baldocchi et al., 2003). The Eddy Covariance (EC) technique can measure three components of the ecosystem carbon cycle, net ecosystem exchange (NEE), gross primary productivity

(GPP) and total ecosystem respiration (TER). Some definitions follow (Chapin et al., 2006):

NEE: The exchange of carbon (in the form of CO₂) between the land biosphere and the atmosphere over a specified period of time is referred to as the net amount of carbon exchanged. When the value of NEE is negative, it indicates that the land biosphere has taken up carbon, whereas a positive value suggests that the land biosphere has released carbon.

NEP: The Net Ecosystem Productivity (NEP) is the inverse of NEE, which means that NEP's positive and negative values indicate carbon absorption and release by the biosphere, respectively.

GPP: This refers to the aggregate quantity of carbon that is transferred between the Earth's land-based ecosystems and the atmosphere by means of photosynthesis.

NPP: Net primary productivity; GPP - autotrophic respiration which includes growth and maintenance respiration.

TER: This is a collective term for autotrophic, heterotrophic, microbial, and soil respiration, represents a portion of the overall carbon absorbed through photosynthesis that is subsequently released back into the atmosphere.

The following equation relates NPP, GPP and RA by definition:

$$NPP = GPP - RA \quad (1)$$

Multiple studies have endeavoured to approximate the AWB in forest ecosystems by utilising allometric models that make use of biometric data such as tree diameter at breast height (DBH), tree height, tree age, and forest distribution. These biometric data are gathered as part of national forest inventory programs or surveys, but due to their resource-intensive nature, such surveys are infrequent and record only five-yearly or decadal changes in forests (Evans et al., 2022). On the other hand, tree-rings offer a comprehensive estimate of annual AWB increment as they record tree growth data on an annual resolution. Trees in temperate regions produce a light-coloured wood, earlywood, and a dark-coloured wood, latewood, during the distinct growing season (Robinson et al., 1989). These rings can be easily identified by the naked eye. However,

identifying annual rings for tropical trees is challenging as they lack distinct growing seasons. Nevertheless, efforts are being made to incorporate microscopy to distinguish growth seasons using anatomical features such as vesicles, cell walls, and cell number density of the cells to identify the tree rings (Nath et al., 2016). Once the annual rings are identified, their widths are measured, and an annual series is recorded. These measurements are then standardised, and an annual basal area increment (BAI) index can be reconstructed. The density of the rings can also vary annually depending on the climate and tree physiology, and for early and late woods, tree ring density is also utilised as a tree growth index.

Studies utilising allometric models incorporating tree ring indices and ecosystem parameters measured by flux towers have gained popularity in estimating AWB (Babst et al., 2013, Klesse et al., 2018 and Cabon et al., 2020). However, most of these studies have been limited to temperate zones where there is an abundance of tree-ring data and flux tower sites. In India, carbon sequestration and AWB estimation studies have primarily utilised methods such as forest inventories and destructive sampling (Mani and Parthasarathy, 2007), high-resolution remote sensing data (Waltham et al., 2020), ecosystem modelling (Deb Burman et al., 2017), Eddy covariance ecosystem carbon flux data (Waltham et al., 2017, Deb Burman et al., 2020, and Rodda et al., 2021), and a combination of remote sensing, vegetation models, and forest inventory data (Fararoda et al., 2021). Nevertheless, the potential of tree-ring indices from sub-tropical India as proxies for estimating ecosystem productivity remains unexplored. Thus, this study aims to investigate the potential of tree-ring indices in sub-tropical India for estimating ecosystem productivity.

Dendrochronological proxies have been extensively used to reconstruct climate variables such as rainfall and temperature over the last 400-500 years (Borgaonkar et al., 1999). In this study, we aim to investigate the potential of these proxies as indicators of ecosystem productivity for the recent past (1850-1990) using available records. Unfortunately, the tree-ring data available did not overlap with the time period for which remote sensing or observation-based ecosystem productivity data was available over

the Indian region. However, we took this as an opportunity to test the performance of the proxy for the longest time period available from models of the sixth phase of the Coupled Model Intercomparison Project (CMIP6). To this end, we test the following sub-hypotheses: (1) outputs from historical experiment simulations from selected CMIP6 models can be used as a record of ecosystem productivity for the historical period (1850-2014), and (2) tree-ring indices are a good proxy for subtropical forests in India.

To test hypothesis (1), we compare the model outputs with existing remote sensing and flux tower records over selected regions in India. To test (2), we compute statistical measures to indicate a correlation between the indices and model outputs. Furthermore, the performance of the proxies is tested by studying the relationship between the ecosystem variables and tree-ring indices in the presence of other climate variables that affect carbon allocation in trees. It should be noted that the study does not aim to establish a one-to-one correspondence between tree-ring indices and ecosystem carbon flux variables.

Data and Methods:

2.1.1. CMIP6 Model data

This study utilised model outputs from the Coupled Climate Carbon Cycle Model Intercomparison Project (C4MIP) (Jones et al., 2016), an intercomparison project endorsed by the Coupled Model Intercomparison Project Phase 6 (CMIP6) (Eyring et al., 2016) under the World Climate Research Program (WCRP). The model outputs were obtained from the open-access Earth System Grid Federation (ESGF) [website](#). They were selected from two CMIP6 models, ACCESS-ESM1-5 and NorESM-LM2, based on their similar initialisation, forcings, physical parameters, and carbon cycle model traits for the historical-biogeochemical (hist-bgc) experiment.

Table 2.1 briefly describes the treatment of the carbon cycle, vegetation modelling, and land use changes for the models (Seland et al., 2020, Lawrence et al., 2019 and Zeihn et al., 2020). The model output for GPP, NPP, and RA was downloaded for the entire globe. Still, as these were coupled Earth System Models (ESM), their spatial resolution was coarse (see Table 2.1). The model outputs needed to be upscaled to a finer resolution to investigate the association between local tree ring sites and model outputs.

Climate Data Operators (CDO), a public licence software developed at the Max Planck Institute for Meteorology (MPI-M), Germany (Schulzweida, 2022) was used to regrid and sub-set the model outputs to the Indian subcontinent region. The CDO function "remapcon" was used to regrid the model outputs to a $1^\circ \times 1^\circ$ grid, conserving flux quantities in each grid cell. The data was then subset to a latitude-longitude box of 68°E - 95°E and 8.5°N - 40.5°N . The model outputs were available as monthly means of carbon fluxes in the unit of $\text{kgC m}^{-2} \text{s}^{-1}$, which was converted to a daily carbon flux unit of $\text{gC m}^{-2} \text{d}^{-1}$ and then to monthly sums of GPP, NPP, and RA by multiplying by 30 (average days in a month).

Model	ACCESS-ESM1.5	NorESM2-LM
Resolution	latitude x longitude = 1.25° x 1.87°	latitude x longitude = 1.89° x 2.5°
Radiative forcing	In concentration-driven, spatially constant, using the global mean data of Meinshausen et al. (2017). Land use changes are prescribed. Solar forcing is provided as irradiance forcing.	In emission-driven experiments (e.g. esm-piControl), CO2 is an interactive 3D tracer coupled to terrestrial and marine fluxes and anthropogenic emissions.
Vegetation	Evolves dynamically Static vegetation coverage - 13 surface vegetation types/tiles: evergreen needleleaf, evergreen broadleaf, deciduous needleleaf, deciduous broadleaf, shrub, C3 grass, C4 grass, tundra, crop, wetlands. Vegetation fractions in each tile vary with time through prescribed files. Resolution of dataset 0.5° x 0.5° Phenology is determined by latitude and vegetation type. Leaf carbon pool is a prognostic variable.	Vegetation distribution is prescribed from land use datasets, but vegetation state like LAI etc., is prognostically determined. All PFTs compete for water and nutrients from the same soil column. Vegetation types: evergreen type, for which some fraction of annual leaf growth persists in the displayed pool for longer than one year; a seasonal-deciduous type with a single growing season per year, controlled mainly by temperature and day length; and a stress-deciduous type with the potential for multiple growing seasons per year, controlled by temperature and soil moisture conditions. Phenology is prognostic, responds to soil and air temperature, soil water, day length and management practices.
Carbon cycle	Model - CASA-CNP: Has carbon cycle integrated with nitrogen and phosphorus cycles Prognostic variables: 4 pool cSoil, Vegetation Fractional coverage, LAI and Canopy Height on PFTS. Vegetation carbon pools: Leaf, wood, root, and labile Allocation to these pools is determined by the vegetation type. No forest stand dynamics have been defined No methods specified for maintenance and growth respiration No method is specified for the decomposition of carbon soil.	Model - Carbon cycle in Land model (CLM5): Prognostic variables: vegetation, litter, soil organic matter, all carbon fluxes GPP, NPP, all respiration types, long-term and short-term storage pools. Number of carbon pools: 23 Allocation to the carbon pools is fixed and determined by the PFT. Allocation bins: Leaves, fine roots, coarse roots, stems. No forest stand dynamics were mentioned. Maintenance respiration depends on leaf nitrogen content, PFT and temperature. Growth respiration is calculated as 0.11 factor of total carbon allocation to new growth after allocation to N acquisition.

Table 2.1. Model descriptions of CSIRO’s ACCESS-ESM1.5 and NCAR’s NorESM2-LM

2.1.2. Remote sensing data

The performance of the selected CMIP6 models was evaluated using various sources, including high-resolution remote sensing data. We used the GPP data with an 8-day

resolution from the MOD17A2HGF v.061 product, obtained from NASA's Moderate Resolution Imaging Spectroradiometer (MODIS) project. The data was downloaded using the Application for Extracting and Exploring Analysis Ready Samples (APPEARS) [tool](#) provided by NASA from 2000-01-01 to 2014-12-31. The data was filtered and then rescaled and converted to monthly sums of daily mean GPP in units of $\text{gC m}^{-2} \text{d}^{-1}$.

The spatial average of the data was calculated to create a time series. The North Western Himalayan (NWH) region was selected using a box with latitude and longitude coordinates of 29.5°N to 32.5°N and 77°E to 79°E. The MOD17 product is based on a remote-sensing driven light use efficiency (LUE) model. However, it is important to note that LUE-based models have uncertainty in parameterising the environmental scalars (Waltham et al., 2017).

2.1.3. Eddy Covariance CO₂ flux data

Eddy Covariance technique measure CO₂ fluxes in real-time and are the closest to ground observed data available for variables related to ecosystem productivity (Deb Burman et al., 2021; Sarma et al. 2022). The use of EC technology in India is relatively recent, with only a few site years being available but almost none of these in the public domain. In this study, we use the published results by the Indian Space Research Organisation (ISRO), who analysed the flux data for Betul, a tropical deciduous forest ecosystem in Madhya Pradesh (Rodda et al., 2021).

The EC tower measures the total vertical canopy flux of CO₂ away from the land surface. This measurement can be considered as the NEE if the inorganic oxidation of carbon is negligible and there is no lateral advection below the canopy height (Chapin III et al., 2006). The nighttime measurements are solely due to ecosystem respiration. A temperature-respiration function is obtained from the nighttime data to estimate daytime respiration. It is then added to the flux measured during the day to estimate the CO₂ flux due to primary productivity.

2.1.4. Reanalysis data

We used the reanalysis data to examine the association between the annual tree ring variable and annual aggregates of ecosystem productivity in the presence of other climate factors which affect tree growth. For this purpose, we used ERA5 reanalysis climate data (Hersbach et al., 2023) produced by the Copernicus Climate Change Service(C3S) at the European Centre for Medium-Range Weather Forecasts (ECMWF). We chose this dataset despite its high root mean square error (RSME) and inability to capture extreme events because it presented the longest available climate record from 1959 to the present for the sites of interest, and the product captures the distribution of the climate variables fairly well (Jiang et al., 2020). We used the surface temperature and specific humidity to calculate vapour pressure deficit (VPD) using the following equation:

$$SVP = 610.7 \times 10^{\frac{7.5 \times T_{air}}{273.3 + T_{air}}} \quad (2)$$

$$RH = \frac{SH}{0.623 \times \frac{SVP}{P_{air} - SVP}} \quad (3)$$

$$AVP = SVP \times \frac{RH}{100} \quad (4)$$

$$VPD = SVP - AVP \quad (5)$$

Where SVP - saturation vapour pressure, T_{air} - surface air temperature, RH - relative humidity, SH- specific humidity, P_{air} - atmospheric pressure at surface, AVP - actual vapour pressure

2.1.5. Tree ring data

In this study, we utilised tree ring records of ring width measurements obtained from the International Tree Ring Data Bank (ITRDB) and downloaded from the [World Data Service for Paleoclimatology](#), managed by the National Oceanic and Atmospheric Administration (NOAA). For the Indian subcontinent region, the tree ring width measurements were mainly obtained from NWH sites (marked on Figure 2.1) (Borgaonkar et al., 2004). They covered a few hundred years up to the late 20th

century. Raw ring width measurements for two species from four sites were downloaded. These data were processed using [dplR](#), a dendrochronological package (Bunn, 2008) in R Studios (version: 2022.02.2+485), to create representative chronologies for each site. Details regarding the sites can be found in Table 2.2, and the geographical locations of the sites are displayed on a map of India in Figure 2.1.

Site name	Location	Elevation	Dominant species	no. of trees	no. of cores	Record length
Ghansali (Ghan)	30.6N, 78.75E	800-1200m	<i>Pinus roxburghii</i>	17	26	1796-1990
Jageswar (Jag)	29.5N, 79E	2000m	<i>Cedrus deodara</i>	9	14	1657-1990
Kufri (Kuf)	31N, 77E	2400-2700m	<i>Cedrus deodara</i>	18	34	1775-1988
Manali (Mnl)	32N, 77E	2000m	<i>Cedrus deodara</i>	21	42	1676-1988

Table 2.2 Information on the tree ring sites used in the study.

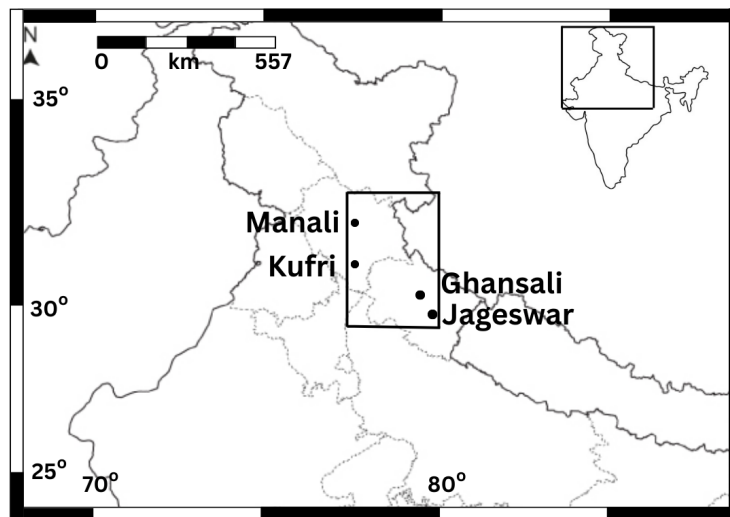


Fig 2.1 Map of northern India showing the tree ring sites used in this study. The boxed region around the sites shows the NWH region used for the regional analysis. Extending from 29.5N to 32.5N and 77E to 79E.

Intra-annual and annual scale data can be recorded through tree rings; however, extracting meaningful signals from this data can be challenging. Various factors such as biological growth effects, tree physiology, external competition, anthropogenic

disturbances near the site, stand distribution and age must be considered. Additionally, Cook et al. (1995) have described the "segment length curse" associated with the tree ring series, which suggests that the series can only capture long-term variability whose wavelengths are smaller than the series. In this study, we focus on the annual growth and increment of woody biomass of trees, and thus a short series is sufficient. Appropriate detrending methods are applied to remove the biological and external effects unique to individual trees from the raw ring width measurements. We evaluated two kinds of detrending methods; a) smoothing cubic splines, which is a stochastic method of passing a low-pass filter represented by a 32% N (total number of observations) cubic spline, it preserves 50% of amplitude variations of 45 years of wavelength (Dietrich and Anand, 2019), and b) a deterministic method, modified negative exponential or a straight line with a negative slope (NELR) where, a modified negative exponential curve is fitted after iterative numerical computation and a straight line is fitted only when there are numerical instabilities in fitting an exponential curve (Helama et al., 2004), for their suitability in preserving tree growth patterns. We also estimated BAI from the raw ring width measurements after standardising them using NELR or a smoothing spline. Similarly, ring width index (RWI) was obtained by fitting NELR or a smoothing spline or a combination of the two to all the cores individually and then standardising the measurements by computing the ratio of the raw measurement and the fitted detrending curve. A site chronology was created using a biweight robust mean (Fonti et al., 2004) of all the standardised measurements. We did not use the more established and frequently used detrending methods to estimate tree-growth (Peters et al., 2015) regional curve standardisation (Esper et al., 2003) or C-method (Biondi and Qeadan, 2008) due to a lack of data on biological factors such as DBH at the time of sampling, distance to pith from the innermost ring, and tree age.

We also recognize that BAI assumes uniform tree growth in concentric circles, which is not always true, especially for trees growing on elevated steep slopes. So an average raw ring width was calculated using all the cores available of the same tree before using the R functions *bai.in* and *bai.out* to estimate the BAI. Several chronologies were constructed a) using the average of two cores, b) using the detrended and standardised

values of the average cores, and c) using one core per tree to test their performance. The formula for calculating BAI given by (Biondi and Qeadan, 2008) is:

$$a_t = \pi r_t^2 - \pi r_{t-1}^2 \quad (6)$$

This formula can also be presented as

$$a_t = w_t^2 + 2w_t R_{t-1} \quad (7)$$

Here w_t is the width of the ring at year t in one direction, R_{t-1} is the tree's radius at breast height in the year previous to t .

The calculation of BAI using the function *bai.in* from the R library *dpIR* also required information about the distance to pith (d2pith) from the innermost ring for which a default value of one year distance from the pith to the innermost ring of the tree was applied by the function.

A regional chronology for NWH was made by first testing the inter-site correlation of different chronologies. The chronology producing the highest correlation among all three sites was chosen for NWH chronology and was constructed by taking a mean of the chronologies made for the three sites.

2.2. METHODS

2.2.1. Pearson correlation

The Pearson correlation coefficient is a statistical measure used to assess the degree of the linear relationship between two continuous variables over time, and its values range between -1 (indicating a negative correlation), 0 (no correlation) and 1 (indicating a perfect positive correlation). The test assumes that the variance of the two datasets is homoscedastic. However, if either of the datasets contains outliers, the correlation test results may be skewed, requiring caution in their interpretation. Our study reports test results along with their significance level. It should be noted that this correlation coefficient only captures linear relationships between two variables. The *Pearsonr*

function from the [Scipy](#) package in Python (Virtanen et al., 2020) was used to calculate the correlation coefficient.

2.2.2. Granger causality test

The Pearson correlation coefficient assesses the strength of the relationship between two variables, but it does not provide any directional information regarding this relationship. The Granger causality test has been developed and widely used to address this limitation in climate studies (McGraws and Barnes, 2018). The test evaluates whether a variable can be used to predict another variable in a time series and establishes causality based on the p-value of the F-test, which should be less than 0.05 to indicate significance. We utilised the R-package [lmtest](#) (Zeileis and Hothorn, 2002) to perform the Granger causality test. (Granger, 1969 and Xie et al., 2019)

2.2.3. Dominance analysis

The present study employed dominance analysis using climate reanalysis data, tree ring indices, and CMIP6 model outputs to investigate the strength of the relationship between ecosystem productivity variables and tree growth indices in the presence of other climatic factors that also impact tree growth. Several alternative methods for multiple regression analysis, such as principal component analysis (PCA), structural equation modelling (SEM), and network analysis (NA), were considered. However, PCA needed to be more robust in identifying linear relationships between predictors and the effect variable. It requires a large number of data points for meaningful interpretation. SEM and NA were not preferred as they necessitated the user to specify a preliminary model before conducting the analysis. In contrast, dominance analysis measures the relative importance of predictors in a piecemeal manner without requiring any predefined association between the factors. The method (Budescu 1993; Azen and Budescu 2000, 2001) was utilised to rank the predictors by their relative importance by calculating the incremental pseudo - R^2 of each predictor when added to a predictor model. Unlike its linear analogue, pseudo - R^2 is computed by a logistic regression which maximises the likelihood of the model through multiple sample sizes from the

observations (Hemmert et al., 2018). It indicates the improvement of the model over the null model (no dependency on any input parameter).

If there are p number of predictors, the analysis computed incremental R^2 for $2^p - 1$ models. Among these, a complete model is one with all the predictors involved in the regression; all the other models are called subset models. The analysis checks for different kinds of dominance statistics: individual dominance (variability explained by the predictor alone), interactional dominance (incremental variability explained by the predictor in the presence of all other predictors), average partial dominance (the average impact that a predictor has when it is available in all possible combinations with other predictors except the combination when all predictors are available); and complete dominance (summarises the additional contributions of each predictor to all subset models). A public-domain python [code](#) was used for the analysis.

2.3. Graphical tools

2.3.1. Taylor diagram

The present study utilises a graphical visualisation methodology to analyse and contrast the associations among equivalent data sets, utilising a reference data set as a benchmark. The graph adopts polar coordinates to represent each data set in the form of (r, θ) . The radial distance r characterises the standard deviation of the test data, while the azimuth angle θ corresponds to the inverse cosine of the Pearson correlation coefficient between the test data and the reference data. Moreover, owing to the geometrical properties of the diagram, the distance between the test and reference data points represents the mean root-mean-square (RMS) deviation between the corresponding values of the test and reference data. The diagram was plotted using a modified version of a public-domain python [code](#) (Taylor, 2001).

Results and Discussion

3.1. CMIP6 model validation

We analysed the regridded CMIP6 model outputs of ecosystem carbon flux, specifically GPP, RA, and NPP, related to primary producers. The performance of these model outputs was evaluated by comparing them to available satellite products and observations. To this end, a Taylor diagram was constructed by plotting the GPP time series results from ACCESS-ESM1.5 and NorESM2-LM from Mar. 2000 to Dec. 2014. The monthly summed GPP product of MODIS (MOD17A2HGF v.061) was used as the reference dataset for this comparison. The GPP time series used for the analysis were spatially averaged data over the NWH region.

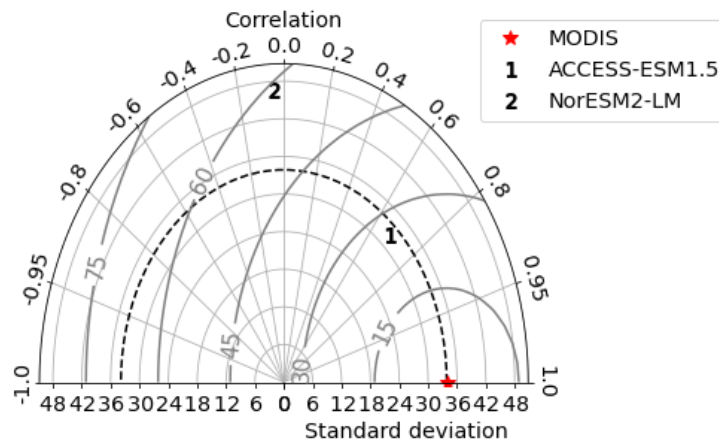


Fig 3.1 Taylor diagram comparing the performance of test datasets of gross primary productivity output from ACCESS-ESM1.5 and NorESM2-LM with MODIS GPP product as reference dataset.

Figure 3.2 shows the multiyear means of monthly ecosystem carbon flux variables, plotted to check the seasonality of both models and the relationship between the variables, NPP, GPP and RA.

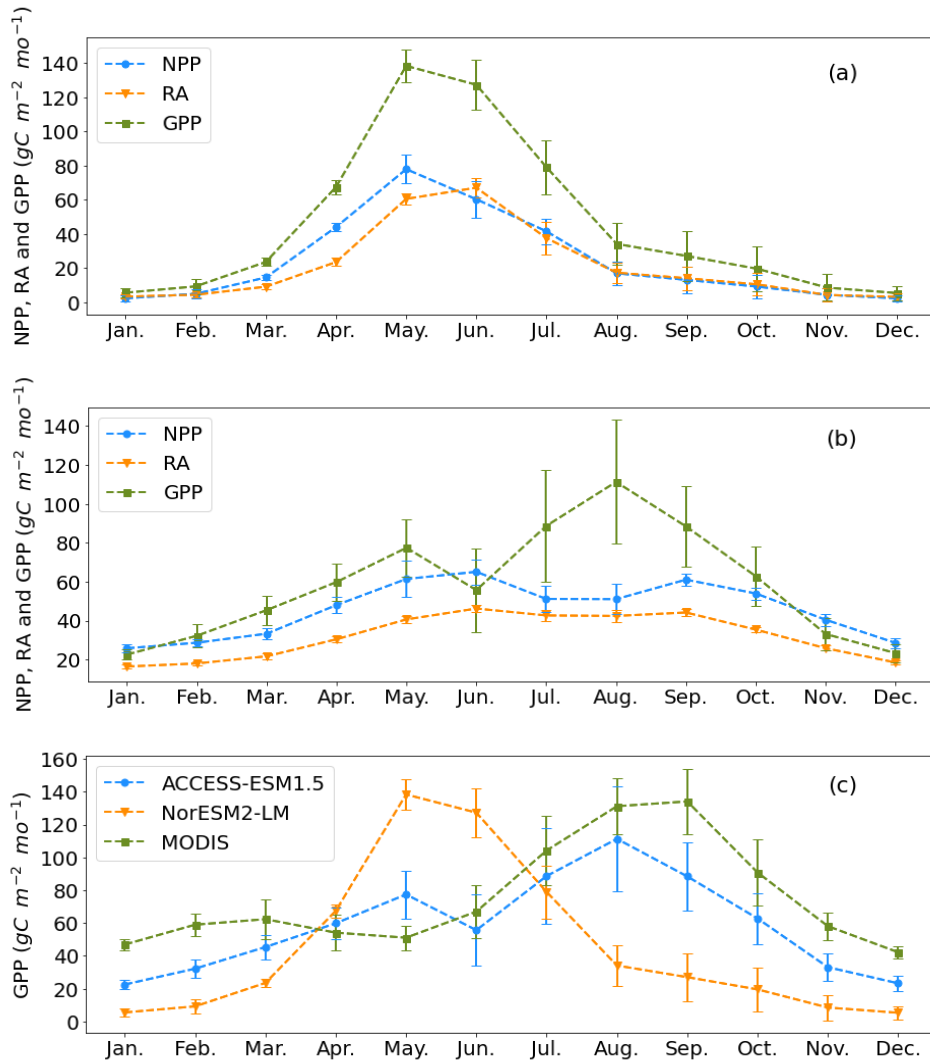


Fig 3.2. Multi-year monthly means from March 2000 to December 2014 for the NWH region of ecosystem carbon flux variables for a) NorESM2-LM CO₂ emissions driven histbgc experiment output, b) ACCESS-ESM1.5 CO₂ concentrations driven histbgc experiment output, c) comparison of ACCESS and NorESM GPP outputs with MODIS GPP product. The y error bars are the standard deviations of each month.

Analysis of the results shown in Figure 3.2 a) and b) indicates the growing seasons that the models simulated. NorESM model outputs suggest that most of the tree growth occurs during the pre-monsoon season (March to May), while ACCESS model outputs show two growing seasons - spring or pre-monsoon (Mar-May) and late monsoon (July to September). In Figure 3.2 c), the performance of the model GPP outputs was tested against the MODIS GPP product. It was observed that the ACCESS model closely replicates the seasonality observed in the MODIS product, while the NorESM model

cannot capture this seasonality. However, it is important to note that there were some discrepancies in the ACCESS-ESM1.5 output where NPP was greater than GPP in a few months (Zeihn et al., 2020). Although there is some uncertainty due to the overlapping standard deviations of NPP, GPP, and RA, it is not physically possible for NPP to be greater than GPP.

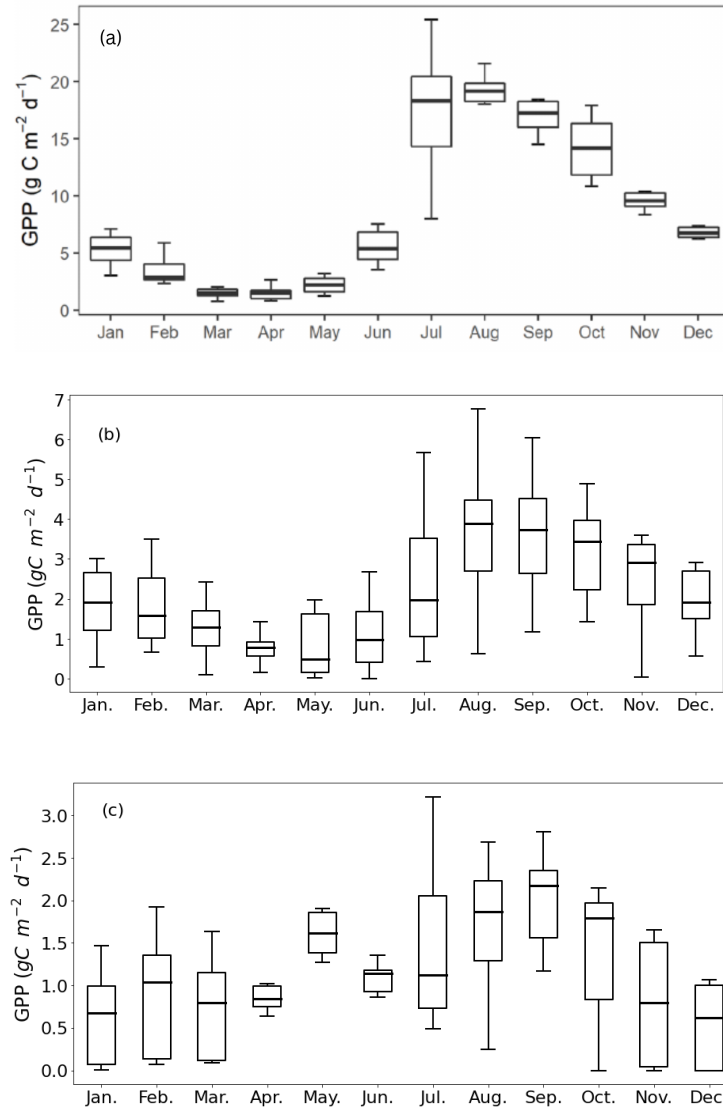


Fig 3.3 Multi-year monthly means of GPP of a forest site in Betul, Madhya Pradesh. (a) GPP data reported by Rodda, et al. 2021. (b) The GPP output from ACCESS-ESM-1.5, and (c) the same from the NorESM2-LM output. The model outputs were extracted from the nearest grid point encompassing the flux tower site.

To further check the performance of the models, we rely on the longest available record of EC data for any Indian forest ecosystem published by Rodda et al. (2021). The authors analysed the carbon sequestration capacity of a mixed-dry deciduous forest in Betul (21.85° N, 77.42° E), Madhya Pradesh, from November 2011 to December 2019 using the CO₂ flux data. Fig 3.3 compares the monthly mean daily GPP of Betul published by the authors and the daily GPP multi-year mean of the same site from the model outputs.

The daily GPP simulated by the models was observed to be smaller by one order compared to the measured EC data. Nonetheless, ACCESS-ESM1.5 outperformed NorESM2-LM in simulating the GPP of the recent past. The seasonal pattern of GPP measured by the flux tower at the site closely resembled that simulated by ACCESS-ESM1.5. The results presented in figures 3.1 to 3.3 instil confidence in the performance of the ACCESS-ESM1.5 model, which appears to simulate the recent past more realistically for the Indian region when compared to the NorESM2-LM model. To check if Equation 1 is balanced, we have examined scatter plots between these two parameters (GPP-RA vs NPP) obtained from the two models (Figure 3.4)

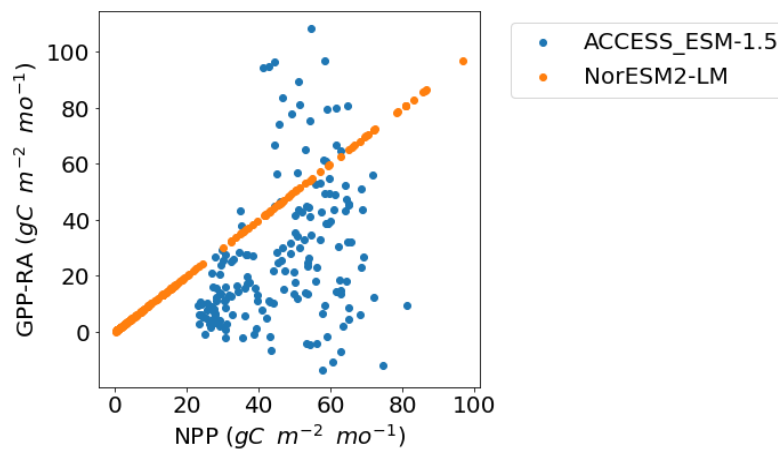


Fig 3.4. A scatter plot of GPP-RA vs NPP for the model outputs from Jan 2000 to Dec 2014 is shown.

NorESM2-LM adheres to Equation 1 consistently from January 2000 to December 2014, whereas ACCESS output treats NPP differently, possibly independent of the relationship between GPP and RA. NorESM2-LM is an emission-driven model in which the carbon model CLM5 prognostically computes all carbon fluxes and the model is also forced by atmospheric CO₂ flux (Lawrence et al., 2019). A flux variable is also

constrained by the condition that it must be conserved locally for every grid cell of the model. This may create a circular issue in the computation of some flux variables (NPP for NorESM in this case). It should be noted that NorESM also fails to model GPP accurately between 1850-1870 and 1890-1910 for the historical period of 1850-2014.

In the ACCESS model, Leaf Area Index (LAI) and GPP are linked together and are prognostic variables. The model was improved from its previous version, ACCESS-ESM1, and the modelling group has modified some parameters in the calculation of GPP and LAI using estimates from the previous model and global observation datasets (Ziehn et al., 2020). However, the model still underestimates LAI and GPP in tropical regions. The carbon model CASA-CNP does not follow Equation 1 for NPP calculation. It uses independent nutrient constraints such as N:C and P:C ratios of leaves, nitrogen and phosphorus content of the soil to control NPP and NEE (Wang, 2009).

3.2. Tree ring analysis

3.2.1. Effect of detrending on tree growth pattern

We have evaluated the RWI and BAI through various detrending techniques and the results are presented in Table 3.1. The association of RWI and BAI with annual accumulations of NPP and GPP from the ACCESS model was analysed for the Ghansali site.

Series name	ACCESS-NPP	ACCESS-GPP
BAI	0.423 (0)	0.2559 (0.002)
BAI after removal of AR1	0.168 (0.046)	0.12 (0.07)
BAI detrended	0.486 (0)	0.228 (0.006)
RWI Spline	0.119 (0.157)	0.043 (0.611)
RWI NELR	0.269 (0.001)	0.181 (0.032)

Table 3.1 Performance of various detrended series as a proxy for tree growth tested against annual sums of NPP and GPP from ACCESS-ESM-1.5, Ghansali site, dominant species – *Pinus roxburghii*. Pearson correlation coefficients are reported for each series and their significance level is mentioned in the brackets.

Pinus roxburghii is categorised as an open-growth, shade-intolerant tree species, which indicates that these trees require sufficient sunlight for their growth, and exhibit an exponential growth phase only during the juvenile period (Borgaonkar et al., 1999). Therefore, the NELR method was employed to detrend the raw measurements. The detrended BAI series exhibited a slightly improved correlation with NPP, the NELR method possibly removes some more biological effects from the BAI index. The BAI series generated was non-stationary and had high autocorrelation (henceforth, AC), as expected from its formulation presented in Equation 7. The correlation of the series with NPP and GPP reduced after the removal of the first-order AC by autoregressive modelling (AR), but the correlation remained significant. Usually in dendroclimatic reconstructions, the AC is removed from the series to capture the high frequency climatic variations (Borgaonkar et al., 1999). However, studies conducted specifically to address the impact of AC on tree growth and age estimation have affirmed that including the positive AC improves tree growth and age estimation (Bullock et al., 2004 and Brienen et al., 2006). AC is defined as the correlation of tree growth during two subsequent time intervals. It can be separated into two components, within-tree AC (temporal correlation within an individual tree) and among-tree AC (correlation among trees after removing within-tree AC) (Brienen et al., 2006). Within-tree AC is controlled by an individual tree's genetic makeup and environmental influences whereas among-tree AC is mainly determined by the size distribution and canopy structure of the forest. Among-tree AC is ecologically meaningful in estimating the stand AWB. However, a more detailed treatment of AC was not possible in this study due to lack of information on the size of the sampled trees. Thus all further analysis was done retaining the autocorrelation in the BAI series.

Cedrus deodara, on the other hand, is a shade-tolerant species, and the growth curve of each tree is unique to the competition for light they experience (Earle, 2023). Therefore, these time series were detrended using a cubic spline with a 45-year wavelength of before further analysis. The statistics of the BAI indices from the study sites are presented in Table 3.2.

Site	Mean BAI (m ²)	SD (m ²)	SE (m ²)	Avg annual change (m ²)
Ghansali	4.6e-4	2.28e-4	1.93e-5	9.17e-5
NWH region	8.28e-4	3.45e-4	2.92e-5	1.71e-4

Table 3.2 BAI statistics from the study sites. Mean, standard deviation (SD), standard error (SE) and average year to year change in BAI are listed.

3.2.2. Comparison of RWI and BAI as tree growth indicators

Table 3.1 results show that the BAI exhibits strong correlations with variables related to ecosystem productivity as compared to the RWI. From Equation 7 we see that basal area increment at year t , BAI_t , is dependent on the ring width of that year (w_t) and the overall radial growth till that year, R_{t-1} . So, BAI_t becomes a linear function of tree size R_{t-1} when w_t is constant. Studies comparing different detrending methods to detect long-term growth trend in trees confirm that BAI performs better than the conventional ring width detrending methods stating it is more sensitive and accurate in capturing long-term growth trends (Peters et al., 2015; Dietrich and Anand, 2019). In this study, tree growth indices are utilised as proxies for estimating carbon fluxes within the ecosystem, which are closely related to the volume and mass increment in forest stands. Studies that used allometric models to estimate AWB have employed formulations similar to Equation 7, where the AWB depends on the tree's diameter at breast height and height (Mani and Parthasarathy, 2007). Several studies have suggested that BAI is a superior indicator of AWB accumulation, as it minimises biological growth trends (Dhyani et al. 2022; Pompa-Gracia et al. 2016).

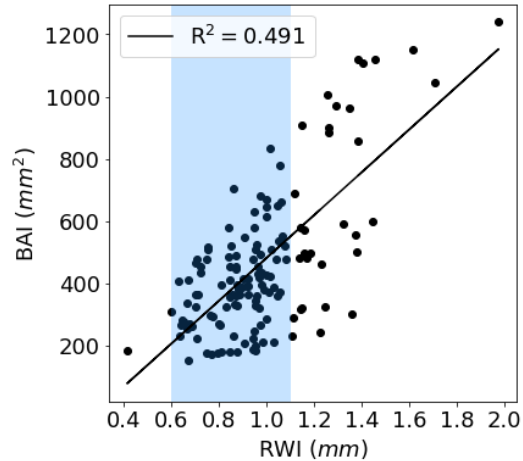


Fig 3.5. Basal area increment and ring width index plotted for Ghansali. When ring width is small (0.6 to 1.1 mm) BAI remains reasonably constant. Points outside the shaded region, below the trendline represent the juvenile phase when BAI is less due to small tree size.

3.2.3. Results from Ghansali

Figure 3.6 shows the Z-score standardised values of detrended BAI, RWI, and GPP from the Ghansali site. The BAI series exhibits a positive trend with a slope of 4.54. It is worth mentioning that the positive peak at the end of the series is also influenced by the detrending method, as indicated in Figure 3.7. Nevertheless, a significant peak (from 1960 - 1980) is present in all the Ghansali cores, suggesting a common strong signal mainly caused by some environmental influence is retained in the chronology. This contributes to the positive trend observed in the BAI series. The lack of biometric information, such as distance to pith from the innermost tree ring in the cores, DBH, and tree age, might have introduced systematic errors in the BAI estimation, which could also contribute to the positive trend in BAI. We observe a one year lag of GPP when compared with BAI (i.e., BAI is affected by the previous year GPP as well) which is further supported by the granger causality test (see Table 3.3). However, this lag is not visible when GPP is compared with BAI Ar1 where autoregressive modelling removes the effect of tree size from the series.

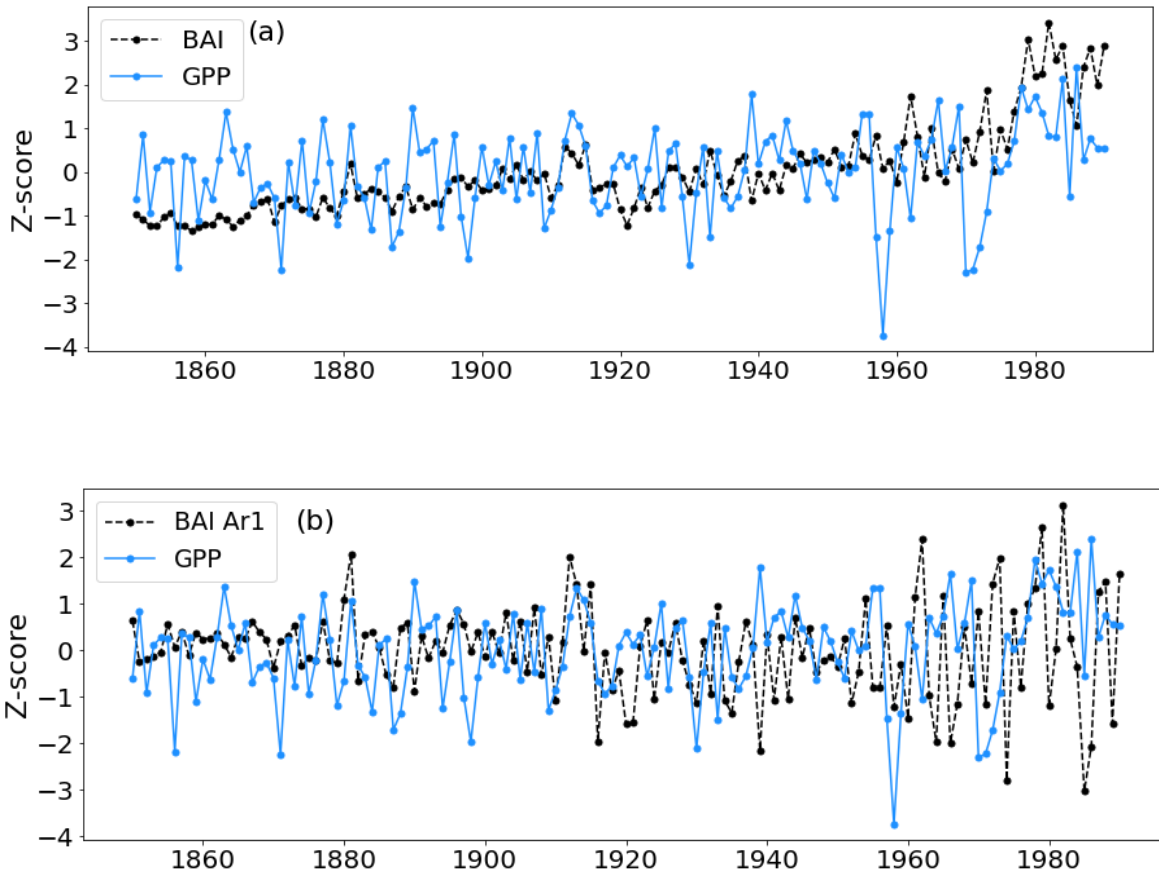


Fig 3.6 a) BAI and annual ACCESS GPP plotted to check overall correlation between the series. b) BAI residual after autoregressive modelling (BAI Ar1) and annual ACCESS GPP. A one-year lag can be noticed in (a) but not in (b).

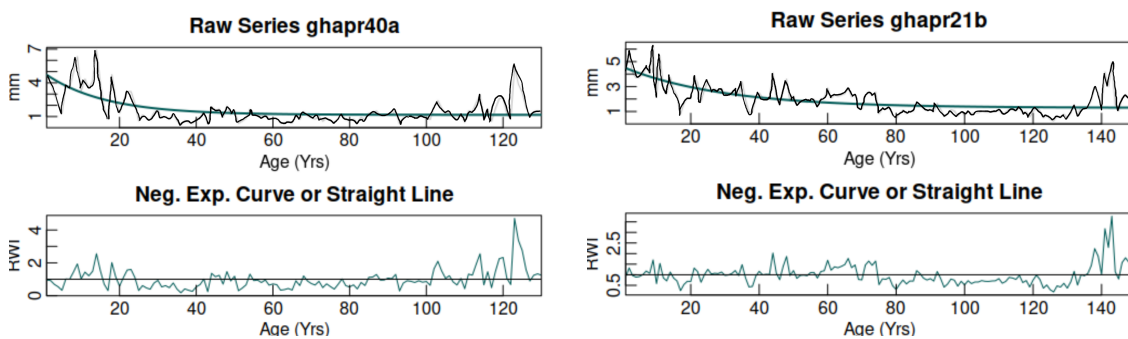


Fig 3.7 Two sample cores from Ghansali showing the increased peak at the end and the standardised values below. The raw series are overlapped with a blue curve showing the NELR curve fitted for detrending the series. Detrending by the ratio method leaves an end effect on the index (Helama et al., 2004).

In Table 3.1, the NPP from the ACCESS model exhibits a strong positive correlation with the tree ring chronologies, significantly higher than the GPP. However, it is possible that this high correlation may be due to erroneous NPP values obtained for the Ghansali region (refer to Fig 3.8). Zeihn et al. (2020), identified the estimation of carbon fluxes such as NPP and NEE as one of the limitations of the ACCESS model. The calculation timescales for ecosystem respiration variables are daily, whereas, for GPP and LAI, it is hourly, which may lead to inconsistencies in the calculation of NPP and NEE. Therefore, despite the significant association of NPP with BAI and RWI, only the GPP output from the ACCESS model is used for comparison with tree ring indices.

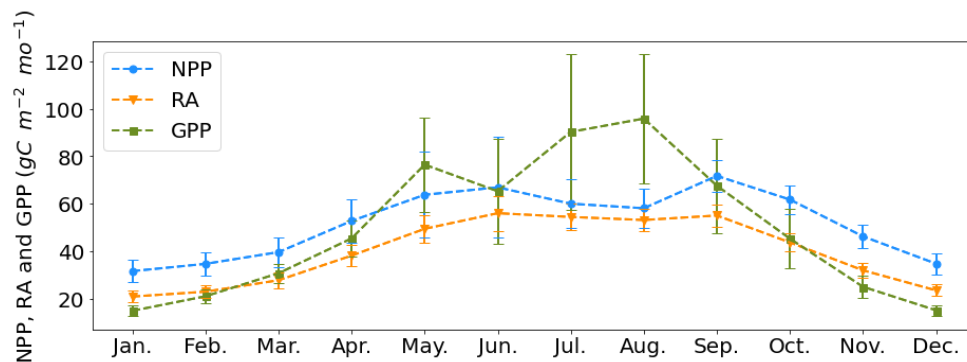


Fig 3.8 Multi-year monthly mean of NPP, GPP and RA values from ACCESS-ESM1.5 for Ghansali for the period 2000-2014.

Further, we conducted a Granger causality test (refer to Table 3.3) to check if there is a directionality to the association between ecosystem carbon flux and carbon assimilation by the dominant forest trees. In this study, GPP was a Granger cause for the carbon assimilation proxies, RWI and BAI, when lagged by one year. However, the association was more significant for BAI, as expected. The reverse Granger tests did not return significant results, indicating that the association between GPP and tree growth indices is unidirectional. Previous studies have also recognised a distinct one-year lag between net ecosystem productivity and tree biomass increment (Teets et al., 2018 and Cabon et al., 2020).

Series	Gpp ~ RWI	GPP ~ BAI	BAI ~ GPP	RWI ~ GPP
Lag order	1	1	1	1
F-test	3.62	9.57	1.90	2.58
P-value of F test	0.056	0.002	0.17	0.11

Table 3.3 Granger causality test results for the Ghansali site.

Figure 3.9 illustrates the monthly correlations with GPP values and annual RWI and BAI of trees. The months that exhibit a significant correlation with the tree ring chronologies are referred to as the growing season months (shaded region), as the variations in these months are closely linked to the tree's growth during that year, and hence considered the peak growing months for the trees. The results suggest that the months from December to March have a negative impact on the trees' growth. In the model, GPP is determined by the water availability in a particular month. During periods of extreme water stress, plant productivity is almost zero, as indicated by the red curve in Figure 3.9. However, evergreen trees can still assimilate carbon for maintenance during such periods, which is not accurately captured by the model. Moreover, winter may also be the wood-producing season for certain woody shrubs such as Ericaceae, Himalayan Nettle, and Banj Oak, which usually occur with Chir Pine trees. These shrubs flower during late spring to early summer and hence may have a high productivity phase during winter, which the model's vegetation tiles may capture (USDA, 2023). Additionally, shrubs are more sensitive to the availability of soil water, which begins to replenish due to snow/glacier melt from early spring, and hence they start growing earlier than Chir Pine trees.

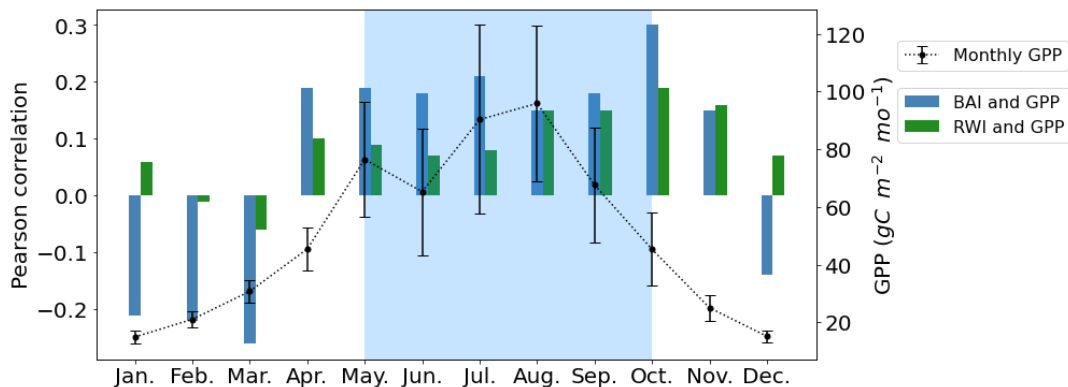


Fig 3.9 Growing season of *Pinus roxburghii* is indicated by the high positive correlation of the month's GPP with the annual tree ring index (BAI or RWI).

Tree growth is significantly influenced by various climatic factors, such as rainfall, temperature, shortwave radiation (SWR), soil water, and VPD. Dendrochronology has been widely used to reconstruct such climate variables for the pre-industrial era (Borgaonkar et al., 1999). To assess the relative importance of different climatic factors on tree growth dynamics and their potential impact on estimating ecosystem productivity from tree-ring indices, we performed a dominance analysis. The results are presented in Figure 3.10, which shows the overall importance of the variables, and Table 3.4, which lists the different types of dominance exhibited by the variables.

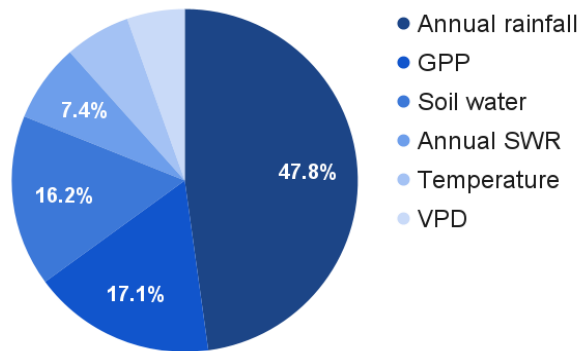


Fig 3.10 Relative importance of variables in explaining the variance in BAI for Ghansali. The ERA5 reanalysis product from 1959-1990 is used to source climate data. The analysis is done for the period 1959-1990. Temperature, VPD and soil water were computed as annual means, whereas rainfall and SWR were computed as annual sums.

Variable	Interactional dominance	Individual dominance	Avg partial dominance	Total dominance	Relative importance (%)
Annual rainfall	0.164	0.1839	0.177	0.176	47.82
GPP	0.072	0.069	0.059	0.063	17.11
Soil water	0.077	0.026	0.063	0.059	16.16
Annual SWR	0.003	0.024	0.034	0.027	7.35
Temperature	0.007	0.053	0.019	0.022	6.15
VPD	0.009	0.046	0.016	0.02	5.4

Table 3.4 Incremental pseudo R^2 (% variance explained) values of each variable when added to regression models. BAI was the target variable. The climate variables and GPP explained 37% of the variance for BAI.

Pinus roxburghii, also known as Chir Pine, is predominantly limited by water availability (Earle, 2023). Our findings indicate that the dominant variables for Chir Pine growth,

apart from GPP, are annual rainfall and average soil water content, which exhibit high interactional dominance, indicating their interdependence. This suggests that ring widths and BAI are highly sensitive to the amount of rainfall received, and a lack of adequate rainfall can significantly impact carbon sequestration by the ecosystem. Additionally, high rainfall is likely to reduce the frequency of forest fires, which are otherwise typical in the Ghansali site, given its proximity to human settlements and susceptibility to fires during dry seasons. The growth of Chir Pine trees is not particularly sensitive to the amount of SWR received in a year since these trees are shade-intolerant. The trees grow independent of the excess amount of sunlight after achieving a threshold amount. The strong influence of rainfall on tree growth patterns highlights the need to apply appropriate climate statistics to ring indices before combining records from different sites for regional analysis of tree growth using regional chronologies (Briffa et al., 1998).

3.2.4. Regional analysis with a different species

To account for the diverse responses of different tree species to climate factors and their associated growth patterns, we selected three sites in the NWH region where *Cedrus deodara* was the dominant species. Dendrochronologists have widely used *Cedrus deodara* to reconstruct past climate in the Himalayan region due to their higher elevation range of 2000m - 3500m, which reduces their susceptibility to anthropogenic activities and increases their sensitivity to climate change (Borgaonkar et al., 1999). The inter-site Pearson correlations between the selected sites are presented in Table 3.5 demonstrate a high coherence in tree growth patterns. Consequently, we combined the sites to construct a regional chronology of BAI and RWI.

Site pair	Detrended BAI correlation
Jag - Kuf	0.608 (0)
Kuf - Mnl	0.862 (0)
Mnl - Jag	0.621 (0)

Table 3.5 Inter-site Pearson correlations of the *Cedrus deodara* trees

The examination of the output from the ACCESS model for the NWH region (as shown in Figure 3.2 b) indicates that the model does not exhibit significant inconsistencies in the calculation of NPP, unlike what is observed in the case of Ghansali. We utilised the annual NPP series for the NWH region to interpret the results. We determined the Pearson correlation coefficients between the detrended BAI chronology of the sites and the NWH region with the annual NPP and GPP series of the sites, which are presented in Table 3.6.

Site name	ACCESS-NPP	ACCESS-GPP
Jag	0.414 (0)	0.134 (0.112)
Kuf	0.576 (0)	0.252 (0.002)
Mnl	0.462 (0)	0.241 (0.004)
NWH	0.509 (0)	0.202 (0.02)

Table 3.6 Pearson correlation coefficients of the individual sites with their annual NPP and GPP and of the NWH region with the regional average of the annual NPP and GPP series. Significance values are mentioned in the brackets.

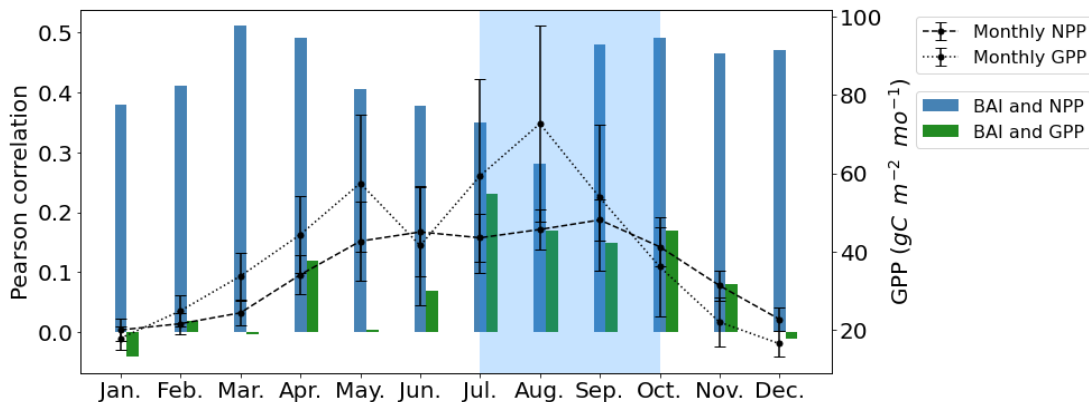


Fig 3.11 Pearson correlation of monthly NPP and GPP with annual BAI.

In Figure 3.11, the monthly correlation with annual BAI is presented to identify the growing season months. A positive correlation indicates that the productivity of that month contributes to the tree stem growth. Conversely, a negative correlation suggests that the productivity of that month is utilised in other parts or processes of the tree, or the ecosystem productivity has a significant microbial contribution, which may not align with tree growth. For *Cedrus deodara*, the pre-monsoon season is a critical growth phase (Dhyani et al., 2022). The monsoon season may increase soil microbial activity, leading to a decrease in NPP and, hence, a low correlation for July and August.

Additionally, we observe that the winter months are also critical in the growth of Deodar trees.

We investigate the influence of various climatic factors on the growth patterns of trees in the NWH region, particularly in relation to BAI and RWI. We performed dominance analysis to determine the key climate variables, and a spatial average of the climate data from the ERA5 reanalysis product was taken over the region. This was done because of the similarity in climatic conditions among the three sites, which were situated at an average elevation of 2200m.

Deodar trees are classified as shade-tolerant and prefer deep and well-drained soils. Their growth is positively affected by high levels of atmospheric moisture, while extremely low temperatures pose a risk to the growth of young trees (Earle, 2023). BAI is considered a more reliable growth indicator than RWI, although it may be less sensitive to variations in climate (Peters et al., 2015).

In Table 3.7 (a), the dominant variables influencing the growth patterns of trees, with BAI as the target variable, are presented. NPP emerges as the most dominant variable, possibly due to the loss of common climate signals in the regional average of the BAI index. However, the climate variables related to moisture, such as precipitation and soil moisture, rank next in order, indicating the sensitivity of tree growth to moisture availability.

In Table 3.7 (b), the results of the dominance analysis for the regional RWI as the target variable are presented, highlighting the climate dependencies of tree growth. The analysis reveals that tree growth is most sensitive to the average annual VPD and soil water and is also influenced by temperature, in addition to the ecosystem productivity. The extremely low dominance of annual rainfall for predicting RWI requires further investigation with site specific information on proximity to an aquifer or river and geographic terrain.

Variable	Interactional dominance	Individual dominance	Avg partial dominance	Total dominance	Relative importance (%)
NPP	0.20	0.218	0.225	0.22	62.3
Annual rainfall	0.059	0.017	0.046	0.043	12.28
VPD	0.011	0.038	0.046	0.039	11.05
Temperature	0.006	0.023	0.034	0.027	7.78
Annual SWR	0.024	0.002	0.022	0.019	5.35
Soil water	0.006	0.0001	0.005	0.004	1.25

Table 3.7 (a) Incremental pseudo R^2 (% variance explained) values of each variable when added to regression models. BAI was the target variable. The climate variables and NPP explained 35% of the overall variance for BAI.

Variable	Interactional dominance	Individual dominance	Avg partial dominance	Total dominance	Relative importance (%)
VPD	0.084	0.097	0.078	0.082	28.94
Temperature	0.059	0.078	0.057	0.061	21.33
Soil water	0.07	0.059	0.053	0.056	19.89
NPP	0.028	0.047	0.058	0.051	17.98
Annual SWR	0.054	0.001	0.026	0.026	9.24
Annual rainfall	0.003	0.005	0.009	0.007	2.61

Table 3.7 (b) Incremental pseudo R^2 (% variance explained) values of each variable when added to regression models. RWI was the target variable. The climate variables and NPP explained 28.38% of the overall variance for RWI.

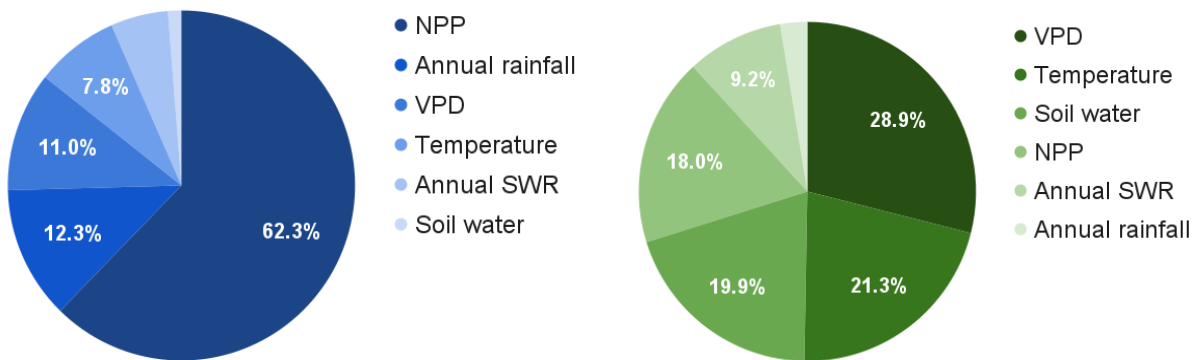


Fig 3.12 Relative importance of variables in explaining the variance in BAI (left) and RWI (right) for the NWH region. The climate data is ERA5 reanalysis data from 1959-1988. The analysis is done for the period 1959-1988. Temperature, VPD and soil water were computed as annual means whereas rainfall and SWR were computed as annual sum.

CONCLUSION AND FUTURE SCOPE

In the present study, we aimed to investigate the potential of tree-ring indices as proxies for ecosystem productivity for Indian subtropical forests. For this, we tested the historical simulation output from two CMIP6 models. CSIRO's ACCESS-ESM1.5 predicted GPP, one of the primary ecosystem carbon fluxes, reasonably well compared to NCAR's NorESM2-LM over the NWH region and the central Indian region. The magnitude of the estimated GPP was low compared to the flux tower observations, but the ACCESS-ESM1.5 GPP showed a good match in capturing the seasonality. We tested the performance of tree-ring indices generated using different standardisation techniques. We found that BAI calculated from the raw ring width measurements was a better indicator of tree growth compared to conventional tree-ring standardisation methods. We found a significant correlation between BAI and the ecosystem productivity variables NPP and GPP for the NWH region and Ghansali, respectively. Furthermore, we found the correlation between the tree index and GPP or NPP to be directional, where NPP and GPP were the granger cause for BAI. We also tested the strength of the association between BAI and NPP or GPP in the presence of other climate variables which affect tree growth by changing the C-allocation to each carbon pool. Annual rainfall significantly impacted BAI apart from GPP for the tree species, *Pinus roxburghii* at the Ghansali site. The BAI index created for NWH regional analysis subdued the regional climatic signals. Thus, we tested the regional RWI for the *Cedrus deodara* species and found that atmospheric moisture availability (VPD), average soil moisture in the column, and air temperature significantly impacted RWI.

Future Scope

This study relied on data available on public-domain thus was limited by the availability of quality tree-ring data suitable for estimating tree-growth and AWB. Detrending methods have a significant impact on the statistical properties of the tree-ring indices, including the variance range, spectrum, and trend. Additionally, detrending may

introduce other notable characteristics, such as end effects and bias in signal trend (Helama et al., 2004). Thus, testing the performance of tree-ring proxies using better standardisation methods (Peters et al., 2014) would give more credibility to the use of the proxy. For this, tree-ring data need to be supplemented by metadata on the forest distribution, types of trees sampled, tree age, DBH and tree height (Coulthard et al., 2020). In this study we may have overestimated BAI by considering that all samples used were complete tree cores. An investigation of the tree core samples or information on the tree diameter can also help estimate the pith distance and missing rings from partial increment cores (Altman et al., 2016). Having access to forest inventory data would enable us to use allometric models to estimate annual increment in aboveground biomass. This reconstructed AWB could then be used for a response function analysis (Borgaonkar et al., 1999) and in understanding the contribution of tree biomass increment in the total ecosystem productivity of a forest. In this study we assumed that the tree-ring density remains constant intra-annually and inter-annually. However, this is not the case, the latewood especially increases in density as the tree matures which may introduce biases in estimating AWB (Babst et al., 2013). This study also suffered from poor sample design while collecting tree-ring data. The selective sampling of trees which would be most sensitive to climate change has been flagged by many studies lately. Sampling the entire forest site or randomised selection of trees are proven to produce least biased estimates of tree growth and forest productivity (Nehrbass-Ahles et al., 2014).

The reasonably well prediction of ecosystem productivity by the ACCESS-ESM1.5 model establishes that modelling outputs can be used in gaps where observations are scarce or non-existent. However, an ESM has limitations such as coarse resolution and incorporation of a limited number of vegetation dynamics and PFTs (Wang et al., 2019 and Zeihn et al., 2020). The ESM outputs can be further enriched using regional models which downscale ESM outputs to higher resolutions with more observations and detailed processes (Gutowski Jr, et al., 2016).

REFERENCES

- Altman, J., Doležal, J., & Čížek, L. (2016). Age estimation of large trees: New method based on partial increment core tested on an example of veteran oaks. *Forest Ecology and Management*, 380, 82–89.
- Azen, R. (2000). Inference for predictor comparisons: Dominance analysis and the distribution of R² differences. *Dissertation Abstracts International B*, 61/10, 5616.
- Azen, R., Budescu, D. V., & Reiser, B. (2001). Criticality of predictors in multiple regression. *British Journal of Mathematical and Statistical Psychology*, 54, 201–225.
- Babst, F., Bouriaud, O., Papale, D., Gielen, B., Janssens, I. A., Nikinmaa, E., ... Frank, D. (2013). Above-ground woody carbon sequestration measured from tree rings is coherent with net ecosystem productivity at five eddy-covariance sites. *New Phytologist*, 201(4), 1289–1303.
- Baldocchi D. D. (2003). Assessing the eddy covariance technique for evaluating carbon dioxide exchange rates of ecosystems: past, present and future. *Global Change Biology*, 9, 479-492.
- Borgaonkar H. P., Pant G. B., and Kumar K. R. (1999). Tree-ring chronologies from Western Himalaya and their dendroclimatic potential. *IAWA Journal*, Vol. 20 (3), 295-309.
- Borgaonkar, H.P.; Pant, G.B.; Rupa Kumar, K. (2004-08-31): NOAA/WDS Paleoclimatology - Borgaonkar - [Ghansali - PIRO - ITRDB INDI020, Jageswar - CDDE - ITRDB INDI021, Kufri - CDDE - ITRDB INDI012, Manali - CDDE - ITRDB INDI013]. NOAA National Centers for Environmental Information. <https://doi.org/10.25921/3gjjx-r006>. Accessed [28-Aug-2022].
- Biondi F. and Qeadan F. (2008). A theory-driven approach to tree-ring standardisation: Defining the biological trend from expected basal area increment. *Tree-ring research*, vol 64, pp. 81-96.
- Brienen, R. J. W., Zuidema, P. A., & Daring, H. J. (2006). Autocorrelated growth of tropical forest trees: Unravelling patterns and quantifying consequences. *Forest Ecology and Management*, 237(1-3), 179–190.
- Briffa, K. R., Schweingruber, F. H., Jones, P. D., Osborn, T. J., Harris, I. C., Shiyatov, S. G., ... Grudd, H. (1998). Trees tell of past climates: but are they speaking less clearly today? *Philosophical Transactions of the Royal Society B: Biological Sciences*, 353(1365), 65–73.
- Budescu, D. V. (1993). Dominance analysis: A new approach to the problem of relative importance of predictors in multiple regression. *Psychological Bulletin*, 114(3), 542-551.

Bullock, S.H., Turner, R.M., Hastings, J.R., Escoto-Rodríguez, M., Ramírez Apud López, Z. and Rodríguez-Navarro, J.L. (2004), Variance of size-age curves: Bootstrapping with autocorrelation. *Ecology*, 85: 2114-2117.

Bunn, A. G. (2008). A dendrochronology program library in R (dplR). *Dendrochronologia*, 26(2), 115–124.

Cabon A., Kannenberg S. A., Arain A., Babst F., Baldocchi D., Belmecheri S., Delpierre N., Guerrieri R., Maxwell J. T., McKenzie S., Meinzer F. C., Moore D. J. P., Pappas C., Rocha A. V., Szejner P., Ueyama M., Ulrich D., Vincke C., Voelker S. L., Wei J., Woodruff D., Anderegg W. R. L. (2020). Cross-biome synthesis of source versus sink limits to tree growth. *Science*, 376, 758-761.

Chakraborty, S., Tiwari, Y.K., Deb Burman, P.K., Baidya Roy, S., Valsala, V. (2020). Observations and Modeling of GHG Concentrations and Fluxes Over India. In: Krishnan, R., Sanjay, J., Gnanaseelan, C., Mujumdar, M., Kulkarni, A., Chakraborty, S. (eds) *Assessment of Climate Change over the Indian Region*. Springer, Singapore.

Chapin III F. S., Woodwell G. M., Randerson J. T., Rastetter E. B., Lovett G. M., Baldocchi D. D., Clark A. D., Harmon M. E., Schimel D. S., Valentini R., Wirth C., Aber J. D., Cole J. J., Goulden M. L., Harden J. W., Heimann M., Howarth R. W., Matson P. A., McGuire A. D., Melillo J. M., Mooney H. A., Neff J. C., Houghton R. A., Pace M. L., Ryan M. G., Running S. W., Sala O. E., Schlesinger W. H. and Schulze E. D. (2006). Reconciling Carbon-cycle Concepts, Terminology, and Methods. *Ecosystems*, 9, 1041–1050.

Cook ER, Briffa KR, Meko DM, Graybill DA, Funkhouser G (1995) The 'segment length curse' in long tree-ring chronology development for palaeoclimatic studies. *Holocene*, 5, 229–237.

Coulthard, B. L., St. George, S., & Meko, D. M. (2020). The limits of freely-available tree-ring chronologies. *Quaternary Science Reviews*, 234, 106264.

Deb Burman, P.K., Sarma, D., Williams, M., Karipot, A., Chakraborty, S. (2017). Estimating gross primary productivity of a tropical forest ecosystem over north-east India using LAI and meteorological variables. *J. Earth Syst. Sci.* 126, 1–16.

Deb Burman, P.K., Shurpali, N.J., Chowdhuri, S., Karipot, A., Chakraborty, S., Lind, S.E., Martikainen, P.J., Chellappan, S., Arola, A., Tiwari, Y.K., Murugavel, P., Gurnule, D., Todekar, K., Prabha, T.V. (2020)b. Eddy covariance measurements of CO₂ exchange from agro-ecosystems located in subtropical (India) and boreal (Finland) climatic conditions. *J. Earth Syst. Sci.* 129, 43

Deb Burman, P. K., Launiainen, S., Mukherjee, S., Chakraborty, S., Gogoi, N., Murkute, C., Kumar, K. (2021). Ecosystem-atmosphere carbon and water exchanges of subtropical evergreen and deciduous forests in India. *Forest Ecology and Management*, 495, 119371.

Dhyani R., Joshi R., Ranhotra P. S., Shekhar M. and Bhattacharyya A. (2022). Age dependent growth response of Cedrus deodara to climate change in temperate zone of Western Himalaya. *Trees, Forests and People* 8, 100221.

Dietrich, R., & Anand, M. (2019). Trees do not always act their age: size-deterministic tree ring standardisation for long-term trend estimation in shade-tolerant trees. *Biogeosciences*, 16(24), 4815–4827.

Earle C. J. (2023). [The Gymnosperm Database](#).

Evans M. E. K., DeRose R. J., Klesse S., Girardin M. P., Heilman K. A., Alexander M. R., Arsenault A., Babst F., Bouchard M., Cahoon S. M. P., Campbell E. M., Dietze M., Duchesne L., Frank D. C., Giebink C. L., Gómez-Guerrero A., García G. G., Hogg E. H., Metsaranta J., Ols C., Rayback S. A., Reid A., Ricker M., Schaberg P. G., Shaw J. D., Sullivan P. F. and Gaytán S. A. V. (2022) Adding Tree Rings to North America's National Forest Inventories: An Essential Tool to Guide Drawdown of Atmospheric CO₂. *BioScience*, Volume 72, Issue 3, Pages 233–246.

Esper J, Cook ER, Krusic PJ, Peters K, Schweingruber FH (2003) Tests of the RCS method for preserving low-frequency variability in long tree-ring chronologies. *Tree-Ring Research*, 59, 81–98.

Eyring, V., Bony, S., Meehl, G. A., Senior, C. A., Stevens, B., Stouffer, R. J., and Taylor, K. E.: Overview of the Coupled Model Intercomparison Project Phase 6 (CMIP6) experimental design and organisation, *Geosci. Model Dev.*, 9, 1937–1958, <https://doi.org/10.5194/gmd-9-1937-2016>, 2016.

Fararoda, R., Reddy, R. S., Rajashekar, G., Chand, T. R. K., Jha, C. S., & Dadhwal, V. K. (2021). Improving forest above ground biomass estimates over Indian forests using multi source data sets with machine learning algorithm. *Ecological Informatics*, 65, 101392

Fonti, P., & Garcia-Gonzalez, I. (2004). Suitability of chestnut earlywood vessel chronologies for ecological studies. *New Phytologist*, 163(1), 77–86.

GitHub repository for the Taylor diagram code: <https://gist.github.com/ycopin/3342888>

Granger C. W. J. (1969). Investigating Causal Relations by Econometric Models and Cross-spectral Methods. *Econometrica*, Vol. 37, No. 3, pp. 424-438.

Gutowski Jr., W. J., Giorgi, F., Timbal, B., Frigon, A., Jacob, D., Kang, H.-S., ... Tangang, F. (2016). WCRP COordinated Regional Downscaling EXperiment (CORDEX): a diagnostic MIP for CMIP6. *Geoscientific Model Development*, 9(11), 4087–4095.

Helama S., Lindholm M., Timonen M., and Eronen M. (2004). Detection of climate signal in dendrochronological data analysis: a comparison of tree-ring standardisation methods. *Theoretical and Applied Climatology* 79, 239–254.

Hemmert, G. A. J., Schons, L. M., Wieseke, J., & Schimmelpfennig, H. (2018). Log-likelihood-based Pseudo-R² in Logistic Regression: Deriving Sample-sensitive Benchmarks. *Sociological Methods & Research*, 47(3), 507–531

Hersbach, H., Bell, B., Berrisford, P., Biavati, G., Horányi, A., Muñoz Sabater, J., Nicolas, J., Peubey, C., Radu, R., Rozum, I., Schepers, D., Simmons, A., Soci, C., Dee, D., Thépaut, J.-N. (2023): ERA5 hourly data on single levels from 1940 to present. Copernicus Climate Change Service (C3S) Climate Data Store (CDS), DOI: 10.24381/cds.adbb2d47 (Accessed on 20-Sep-2022)

Jain H., Tyagi K., Paygude A., Kumar P., Singh R. K., Kumar M. (2021). Allometric Equations for the Estimation of Biomass and Carbon in the Subtropical Pine Forests of India. *Climate Impacts on Sustainable Natural Resource Management*.

Jiang, Q., Li, W., Fan, Z., He, X., Sun, W., Chen, S. and Wang, J. (2020). Evaluation of the ERA5 Reanalysis Precipitation Dataset over Chinese Mainland. *Journal of Hydrology*, 125660.

Jones, C. D., Arora, V., Friedlingstein, P., Bopp, L., Brovkin, V., Dunne, J., Graven, H., Hoffman, F., Ilyina, T., John, J. G., Jung, M., Kawamiya, M., Koven, C., Pongratz, J., Raddatz, T., Randerson, J. T., and Zaehle, S.: C4MIP – The Coupled Climate–Carbon Cycle Model Intercomparison Project: experimental protocol for CMIP6, *Geosci. Model Dev.*, 9, 2853–2880, <https://doi.org/10.5194/gmd-9-2853-2016>, 2016.

Klesse S., Babst F., Lienert S., Spahni R., Joos F., Bouriaud O., Carrer M., Filippo A. D., Poulter B., Trotsiuk V., Wilson R., and Frank D. C. (2018). A combined tree ring and vegetation model assessment of European forest growth sensitivity to interannual climate variability. *Global Biogeochemical Cycles*, 32.

Lawrence, D. M., Fisher, R. A., Koven C. D., Oleson, K. W., Swenson, S. C., Bonan, G., et al. (2019). The Community Land Model version 5: Description of new features, benchmarking, and impact of forcing uncertainty. *Journal of Advances in Modeling Earth Systems*, 11, 4245–4287.

Mani, S., & Parthasarathy, N. (2007). Above-ground biomass estimation in ten tropical dry evergreen forest sites of peninsular India. *Biomass and Bioenergy*, 31(5), 284–290.

McGraw, M. C., & Barnes, E. A. (2018). Memory Matters: A Case for Granger Causality in Climate Variability Studies. *Journal of Climate*, 31(8), 3289–3300.

Meena, A., Bidalia, A., Hanief, M., Dinakaran, J., & Rao, K. S. (2019). Assessment of above- and belowground carbon pools in a semi-arid forest ecosystem of Delhi, India. *Ecological Processes*, 8(1).

Nath, C. D., Munoz, F., Péliissier, R., Burslem, D. F. R. P., & Muthusankar, G. (2016). Growth rings in tropical trees: role of functional traits, environment, and phylogeny. *Trees*, 30(6), 2153–2175.

Nehrbass-Ahles, C., Babst, F., Klesse, S., Nötzli, M., Bouriaud, O., Neukom, R., ... Frank, D. (2014). The influence of sampling design on tree-ring-based quantification of forest growth. *Global Change Biology*, 20(9), 2867–2885.

Pathak M., Slade R., Shukla P. R., Skea J., Pichs-Madruga R., Üрге-Vorsatz D. (2022). Technical Summary. In: *Climate Change 2022: Mitigation of Climate Change. Contribution of Working Group III to the Sixth Assessment Report of the Intergovernmental Panel on Climate Change* [P.R. Shukla, J. Skea, R. Slade, A. Al Khourdajie, R. van Diemen, D. McCollum, M. Pathak, S. Some, P. Vyas, R. Fradera, M. Belkacemi, A. Hasija, G. Lisboa, S. Luz, J. Malley, (eds.)]. Cambridge University Press, Cambridge, UK and New York, NY, USA.

Pant H. and Tewari A. (2014). Carbon sequestration in Chir-Pine (*Pinus roxburghii* Sarg.) forests under various disturbance levels in Kumaun Central Himalaya. *Journal of Forestry Research*, 25(2), 401–405.

Peters R. L., Groenendijk P., Vlam M. and Zuidema P. A. (2015) Detecting long-term growth trends using tree rings: a critical evaluation of methods. *Global Change Biology* 21, 2040–2054

Pompa-García, M., Hadad, M.A. (2016). Sensitivity of pines in Mexico to temperature varies with age. *Atmósfera* 29, 209–219.

Robinson W.J., Cook E., Pilcher J.R., Eckstein D., Kairiukstis L., Shiyatov S. and Norton D.A. (1989). *Some Historical Background on Dendrochronology, Methods of Dendrochronology Applications in the Environmental Sciences*, Cook E. R. and Kairiukstis L. A. Springer - Science.

Rodda S. R., Thumaty K. C., Praveen M. S. S., Jha C. S. and Dadhwal V. K. (2021). Multi-year eddy covariance measurements of net ecosystem exchange in tropical dry deciduous forest of India. *Agricultural and Forest Meteorology*, 301–302, 108351.

RStudio Team (2020). *RStudio: Integrated Development for R*. RStudio, PBC, Boston, MA URL <http://www.rstudio.com/>.

Sandeep, S., Sivaram, M., Henry, M., & Gammara, J. G. P. (2015). Quality control of tree volume and biomass allometric equations in South Asia. UN-REDD report.

Sarma, D, Deb Burman, P.K., Chakraborty, S., Gogoi, N., Bora, A., Metya, A., Datye, A., Murkute, C., Karipot, K. 2022 Quantifying the net ecosystem exchange at a semi-deciduous

forest in northeast India from intra-seasonal to seasonal time scale. *Agricultural and Forest Meteorology* 314 (2022) 108786.

Seland, Ø., Bentsen, M., Oliví, D., Toniazzo, T., Gjermundsen, A., Graff, L. S., Debernard, J. B., Gupta, A. K., He, Y.-C., Kirkevåg, A., Schwinger, J., Tjiputra, J., Aas, K. S., Bethke, I., Fan, Y., Griesfeller, J., Grini, A., Guo, C., Ilicak, M., Karset, I. H. H., Landgren, O., Liakka, J., Moseid, K. O., Nummelin, A., Spensberger, C., Tang, H., Zhang, Z., Heinze, C., Iversen, T., and Schulz, M.: Overview of the Norwegian Earth System Model (NorESM2) and key climate response of CMIP6 DECK, historical, and scenario simulations, *Geosci. Model Dev.*, 13, 6165–6200

Stocker T. F., Qin D. , Plattner G. K., Tignor M., Allen S. K., Boschung J., Nauels A., Xia Y., Bex V. and Midgley P .M. (2013). IPCC, Climate Change: The physical science basis. (eds) Contribution of working group I to the fifth assessment report of the Intergovernmental Panel on Climate Change 1535 pp.

Schulzweida, Uwe. (2022). CDO User Guide (2.1.0). Zenodo.

<https://doi.org/10.5281/zenodo.7112925>

Taylor, K. E., (2001) Summarising multiple aspects of model performance in a single diagram, *Journal of Geophysical Research*, 106(D7), 7183-7192. <https://doi.org/10.1029/2000JD900719>

Teets, A., Fraver, S., Hollinger, D. Y., Weiskittel, A. R., Seymour, R. S., & Richardson, A. D. (2018). Linking annual tree growth with eddy-flux measures of net ecosystem productivity across twenty years of observation in a mixed conifer forest. *Agricultural and Forest Meteorology*, 249, 479–487.

USDA, Agricultural Research Service, National Plant Germplasm System. 2023. Germplasm Resources Information Network (GRIN Taxonomy). National Germplasm Resources Laboratory, Beltsville, Maryland.

URL: <https://npgsweb.ars-grin.gov/gringlobal/taxon/taxonomydetail?id=28538>. Accessed 5 April 2023.

Virtanen, P., Gommers, R., Oliphant, T. E., Haberland, M., Reddy, T., Cournapeau, D., Burovski, E., Peterson, P., Weckesser, W., Bright, J., van der Walt, S. J., Brett, M., Wilson, J., Millman, J. K., Mayorov, N., Nelson, A. R. J., Jones, E., Kern, R., Larson, E., Carey, CJ, Polat, I., Feng, Y., Moore, E. W., VanderPlas, J., Laxalde, D., Perktold, J., Cimrman, R., Henriksen, I., Quintero, E. A., Harris, C. R., Archibald, A. M., Ribeiro, A. H., Pedregosa, F., van Mulbregt, P. and SciPy 1.0 Contributors. (2020) SciPy 1.0: Fundamental Algorithms for Scientific Computing in Python. *Nature Methods*, 17(3), 261-272.

Wang Y. P., Law R. M., and Pak B.(2009). A global model of carbon, nitrogen and phosphorus cycles for the terrestrial biosphere. *Biogeosciences Discussions*, 6, 9891–9944.

Watham, T., Patel, N. R., Kushwaha, S. P. S., Dadhwal, V. K., & Kumar, A. S. (2017). Evaluation of remote-sensing-based models of gross primary productivity over Indian sal forest using flux tower and MODIS satellite data. *International Journal of Remote Sensing*, 38(18), 5069–5090.

Watham, T., Srinet, R., Nandy, S., Padalia, H., Sinha, S. K., Patel, N. R., & Chauhan, P. (2020). Environmental control on carbon exchange of natural and planted forests in Western Himalayan foothills of India. *Biogeochemistry*.

Xie, X., He, B., Guo, L., Miao, C. and Zhang, Y. (2019) Detecting hotspots of interactions between vegetation greenness and terrestrial water storage using satellite observations *Remote Sens. Environ.* 231 111259

Zeileis A and Hothorn T (2002). “Diagnostic Checking in Regression Relationships.” *R News*, 2(3), 7–10. <https://CRAN.R-project.org/doc/Rnews/>.

Ziehn T., Chamberlain M. A., Law R. M., Lenton A., Bodman R. W., Dix M., Stevens L., Wang Y. and Srbinovsky J.(2020). The Australian Earth System Model: ACCESS-ESM1.5. *Journal of Southern Hemisphere Earth Systems Science*, 70, 193–214.